Light-Induced Cooperative Electron–Proton Transfer in Hydrogen-Bonded Networks of *N,N*-Diaryl Substituted 1,4-Bisimines and *meso*-1,2-Diaryl-1,2-ethanediols

Michael Felderhoff, Tanja Smolka, and **Reiner Sustmann***

Essen, Institut für Organische Chemie der Universität

Ingo Steller, Hans-Christoph Weiss, and **Roland Boese***

Essen, Institut für Anorganische Chemie der Universität

Received July 27th, 1999

Keywords: Cooperative effects, Crystal engineering, Electron transfer, Hydrogen bonds, Photochromism

Abstract. The 1:1 cocrystallization of 1,4-diaryl-1,4-bisimines (Ar–CH=N–CH_2-)$_2$ **4**–**11** and substituted *meso*-1,2-diaryl-1,2-ethanediols **1**–**3** leads to supramolecular structures in which the diol is hydrogen bonded by one of its hydroxy groups to an imine nitrogen atom of a 1,4-bisimine. The second functionality in each molecule leads to the generation of ladderlike polymeric structures where each molecule of the diol is linked to two molecules of the 1,4-bisimine and *vice versa*. If the diol carries electron donor groups in the aromatic residue and the 1,4-bisimine correspondingly acceptor groups, then charge transfer interactions are observed. The excited CT complex which corresponds to a radical ion pair is stabilized by migration of a proton of a hydroxy group to the nitrogen atom of an imino group. This is supported by the appearance of a N–H vibration in the IR spectra. The reorganization is also accompanied by changes in the UV/Vis spectra and by the generation of paramagnetism in the crystalline material. The results represent a type of photochromism which has its origin in a light-induced cooperative electron–proton transfer. The photochromism is thermally reversible.

Supramolecular structures which are held together by hydrogen bonds play an important role in chemistry and biology. The cooperativity of many weak interactions creates structures essential for life processes [1]. The understanding of these interactions is one of the pillars of supramolecular chemistry [2]. Crystal engineering on the basis of hydrogen bonding is an area presently actively investigated [3]. The design of hydrogen-bonded networks presents a challenge which goes beyond the esthetic aspect of beautiful structures [4, 5]. It is the generation of new macroscopic properties which are absent in the individual components that provides the incentive for the preparation of new supramolecular structures. Thus, it is hoped that materials with interesting optical, electrical, or magnetic properties can be realized tailor-made.

Recently, we described a 1:1 cocrystal of *meso*-1,2-diphenyl-1,2-ethanediol and phenazine with a thermally reversible photochromic behaviour which had its origin in a light-induced electron transfer between phenazine molecules [6]. Ladder-like supramolecular networks are generated when the bisimine of ethylenediamine and benzaldehyde or the bisimine of an aliphatic amine with glyoxal undergo 1:1 cocrystallization with *meso*-1,2-diphenyl-1,2-ethanediol [7]. The supramolecular structure in which both components carried aromatic residues aroused our particular interest. The phenyl groups of the bisimine are located in the proximity of phenyl groups of neighbouring *meso*-1,2-diphenyl-1,2-ethanediol molecules, and the angle of tilt between the phenyl groups and their separations indicate favourable edge-to-face interactions [8]. Charge-transfer interactions were suggested for systems with suitably substituted aryl groups positioned closely to each other and such a case was indeed discovered when *meso*-1,2-bis(4-dimethylaminophenyl)-1,2-ethanediol was cocrystallized with bis(4-cyanobenzylidene)ethylenediamine. This was described in a preliminary communication [9]. The complexes displayed a thermally reversible photochromism based on an intermolecular cooperative electron–proton transfer. Here, we report on a systematic variation of donor and acceptor substituents in 4-position of the aromatic residues of *meso*-1,2-diphenyl-1,2-ethanediol and *N,N*-diaryl-substituted 1,4-ethylene-bisimines in order to study the scope and the limitations of the cooperative electron-proton transfer.

Results

The molecules *meso*-1,2-diphenyl-1,2-ethanediol (**1**), *meso*-1,2-bis(4-dimethylaminophenyl)-1,2-ethanediol (**2**), and *meso*-1,2-bis(4-methoxyphenyl)-1,2-ethanediol (**3**) were subjected to cocrystallization with several substituted bis(arylidene)-ethylenediamines. As was found previously only the *meso* diastereomer of the 1,2-

  1436-9966/99/3410X-639 $ 17.50 + .50/0

diols undergoes cocrystallization [7]. Usually the components were dissolved in ethyl acetate in a 1:1 ratio, and these solutions were kept at room temperature allowing the solvent to evaporate slowly. Light sensitive cocrystals were grown in the dark. Not all combinations of the components were introduced into cocrystallization and of those chosen not all cocrystallizations could be realized. Table 1 lists 16 successful cocrystallizations.

Table 1 Cocrystallization of 1,2-Diols **1**–**3** and 1,4-ethylene-bisimines **4**–**11** (+ = successful, – = not successful, blank = not attempted experiments

4–**11**	**1**	**2**	**3**
Ar = C_6H_5 (**4**)	+	+	+
(4)NC-C_6H_4 (**5**)	+	+	–
(4)O_2N-C_6H_4 (**6**)	+	+	–
(4)H_3CO_2C-C_6H_4 (**7**)	+	+	+
(4)F_3C-C_6H_4 (**8**)	+	+	–
(4)$(H_3C)_2N$-C_6H_4 (**9**)	+	–	
(4)H_3CO-C_6H_4 (**10**)	+		–
(4)C_5H_5N (**11**)	+	+	–

Cocrystals of meso-1,2-Diphenyl-1,2-ethanediol (**1**) and *Bisimines* **4**–**11**

Besides 4-donor and 4-acceptor aryl substituted bis(arylidene)ethylenediamines **5**–**10** we examined the heterocyclic bisimine **11** prepared from 4-formylpyridine and ethylenediamine. In each case we isolated crystals which proved to be 1:1 cocrystals of the components. Generally, they show sharp melting points which are between those of the individual components. The 1:1 composition could be demonstrated easily by dissolving the cocrystals and recording a ^{1}H NMR spectrum. The ^{1}H NMR spectrum in deuterochloroform consists of the superposition of the spectra of the components, *i.e*. there is no aggregation detectable, for instance by a change in the chemical shift of the hydroxy protons when compared to their chemical shifts in the spectra of the components. Consequently, the aggregation is a solid state property only. Hydrogen bonds are detected in the IR spectrum of the crystals of *meso*-1,2-diphenyl-1,2-ethanediol [10], but the formation of new hydrogen bonds in the cocrystal manifests itself in the wavenumbers of the OH-vibration. Diol **1** displays two overlapping, rather broad bands at 3 374 and 3 316 cm^{-1}, the cocrystals show a single broad band between 3 211 and 3 282 cm^{-1}.

X-ray analyses of the cocrystals of **1** with **5**–**11** were not carried out as it is very likely that they have a similar structure as the supramolecule from **1** and bis(benzylidene)ethylenediamine (**1**+**4**) [7]. None of these cocrystals showed photochromism on irradiation as an indication of a cooperative electron–proton transfer and also no esr activity could be detected after irradiation.

Cocrystals of meso-1,2-Bis(4-dimethylaminophenyl)-1,2-ethanediol (**2**) *and Bisimines* **5**–**8**, *respectively* **11**

The cocrystal obtained from the 4-dimethylaminophenyl substituted diol **2** and the 4-cyanosubstituted bisimine **5** was the first case showing photochromism [9]. We expected that also cocrystals of **2** and **6**–**8**, respectively **11** might be candidates for charge transfer (CT) interactions and, therefore, might exhibit a cooperative electron–proton transfer. CT interactions are best if the π-systems involved are arranged in parallel planes [11]. The angle of tilt between the phenyl groups of the components in the cocrystal (**1**+**4**) might perhaps be influenced if CT interactions between the aromatic rings are induced. Therefore, we carried out X-ray analyses of the complexes (**2**+**6**) – (**2**+**8**), respectively (**2**+**11**). The arrangement of the molecules in the cocrystal is presented in Figure 1 for (**2**+**6**), the cocrystal with the strongest acceptor group among the bisimines. Figure 2 gives the relative arrangement for some representative examples.

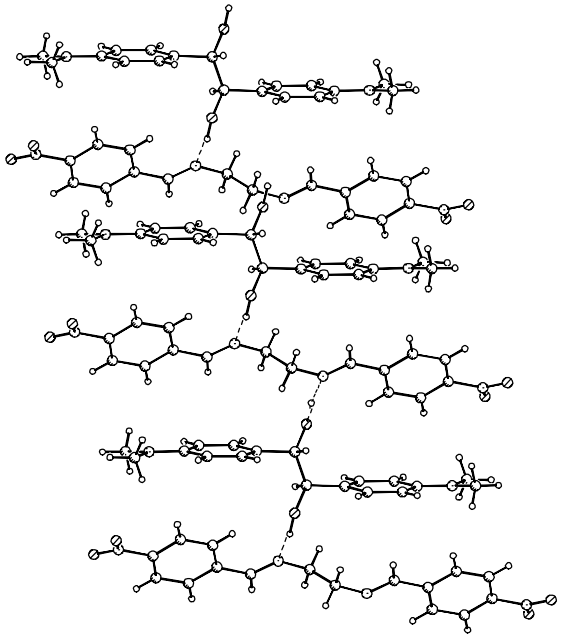

Fig. 1 Crystal Packing of the cocrystal of *meso*-1,2-bis(4-dimethylaminophenyl)-1,2-ethanediol (**2**) and bis(4-nitrobenzylidene)ethylenediamine (**2** + **6**).

Further geometrical data are presented in Table 2, and crystallographic details are given in Table 3. Figure 1 exemplifies the ladderlike structure of the cocrystal (**2** + **6**), each molecule binding to two neighbouring molecules *via* hydrogen bridges. The pairs of bisimine and diol in the cocrystals of Figure 2 have the same arrangement. The phenyl groups in the subunits are coplanar, those of different molecules are tilted to each other by

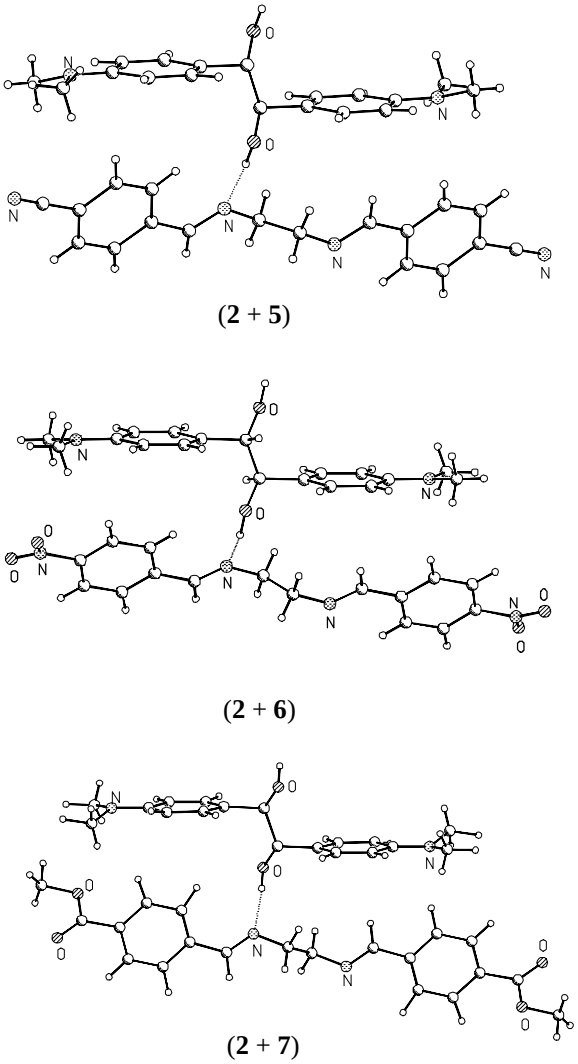

(**2** + **5**)

(**2** + **6**)

(**2** + **7**)

Fig. 2 X-ray structures of photochromic cocrystals of *meso*-1,2-bis(4-dimethylaminophenyl)-1,2-ethanediol (**2**) and 1,4-bisimines **5**–**7**.

angles ranging from 48.8° for (**2** + **6**) to 64.0° for (**2** + **8**). It is tempting to interpret the angle of 48.8° which is found for the combination of **2** with the nitro-substituted bisimine which has the strongest acceptor group in the series as the result of the influence of CT interactions. However, the variation is generally small, and the edge to face interactions seem to be more important than CT interactions. All structures are centrosymmetric which produces local C_i symmetry for each component.

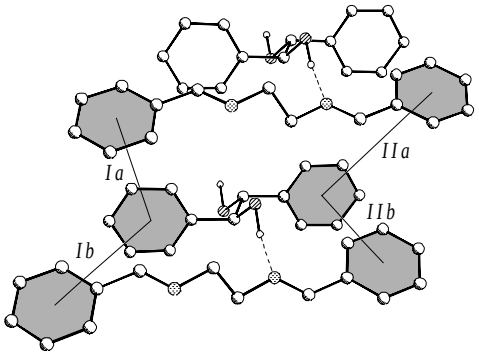

Fig. 3 Aryl-Aryl arrangement in the cocrystal of *meso*-1,2-diphenyl-1,2-ethanediol (**1**) and bis(benzylidene)ethylenediamine (**1** + **4**).

The distance O···N in the O-H···N bridges ranges from 2.84 to 2.91 Å which is normal [13, 14]. The bridges are not completely linear adopting angles of ca. 170° in all cases except for (**3** + **7**) in which the position of the hydrogen atom could not be determined with a sufficient accuracy because of weak diffracting crystals. It should be noted that some of the cocrystals display a disorder with respect to the central part of the diol (see Table 3).

The feasibility of CT interactions depends on the separation and the arrangement of the π-systems. In order to analyse this in more detail the distances between the centroids of the phenyl groups are given in Table 2 (designations see Figure 3). For (**2** + **5**) – (**2** + **8**), respectively (**2** + **11**), and for (**3** + **7**) we find distances between centroids of the aryl substituents within the ladder-like stacks of 4.769 to 5.026 Å (*IIb* in Table 2), and of 5.511

Table 2 Geometrical data for the hydrogen bonds and aryl groups of the cocrystals of *meso*-1,2-(4-dimethylaminophenyl)-1,2-ethanediol with acceptor-substituted bisimines.

Bisimine Aryl–CH=N–CH_2CH_2–N=CH–Aryl Aryl =	Diol	r_{O-N} Å	∢O–H···N	$r_{Aryl-Aryl'}$ [a] Å I		II		∢Aryl–Aryl [b]
				a	*b*	*a*	*b*	
4-CN–C_6H_4 (**5**)	**2**	2.897	165°	5.870	565.5	4.912	4.776	57.9°
4-O_2N–C_6H_4 (**6**)	**2**	2.843	170°	5.324	553.3	552.6	476.9	48.8°
4-H_3CO_2C–C_6H_4 (**7**)	**2**	2.885	164°	5.632	5.511	5.100	4.976	55.4°
4-F_3C–C_6H_4 (**8**)	**2**	2.884	162°	546.8	573.2	5.453	5.023	64.0°
4-C_5H_4N (**11**) [b]	**2**	2.911	171°	5.767	5.606	5.120	4.855	57.1°
4-H_3CO_2C–C_6H_4 (**7**)	**3**	2.839	147°	5.520	5.568	5.387	5.026	60.3°

[a]) centres of aryl groups according to Figure 4: The distances of the centroids in column *a* refer to those between the strings of the hydrogen bonded ladders, those in column *b* within the ladders. [b]) angles between the closest aryl rings according to the distances in column II*b*

Table 3 Crystallographic data for cocrystals (**2** + **5**) – (**2** + **8**), (**2** + **11**), and (**3** + **7**) [12].

Compound	(**2** + **5**)	(**2** + **6**)	(**2** + **7**)	(**2** + **8**)	(**2** + **11**)	(**3** + **7**)
formula	$C_{16}H_{14}N_4O_4$ $\cdot C_{18}H_{24}N_2O_2$	$C_{18}H_{14}N_4$ $\cdot C_{18}H_{24}N_2O_2$	$C_{20}H_{20}N_2O_4$ $\cdot C_{18}H_{24}N_2O_2$	$C_{18}H_{14}F_6N_2$ $\cdot C_{18}H_{24}N_2O_2$	$C_{14}H_{14}N_4$ $\cdot C_{18}H_{24}N_2O_2$	$C_{20}H_{20}N_2O_4$ $\cdot C_{16}H_{18}O_4$
mol. mass (g/cm^{-3})	626.7	586.7	652.8	672.7	538.7	626.7
crystal size (mm)	0.24 ·0.23 ·0.09	0.27 ·0.13 ·0.11	0.26 ·0.22 ·0.13	0.32 ·0.21 ·0.19	0.36 ·0.22 ·0.05	0.23 ·0.15 ·0.11
space group	$P\,\bar{1}$	$P\,\bar{1}$	$P\,2_1/c$	$P\,\bar{1}$	$P\,\bar{1}$	$P\,\bar{1}$
a (Å)	6.146(4)	6.1417(10)	7.306(2)	6.0577(10)	6.2092(4)	5.9503(13)
b (Å)	7.341(4)	7.4690(2)	6.193(2)	7.7789(8)	7.4710(5)	7.6631(12)
c(Å)	17.61(2)	16.866(3)	36.526(10)	18.128(2)	16.0583(11)	17.718(3)
α (°)	83.49(6)	87.54(3)	90	90.450(8)	93.395(2)	92.629(14)
β (°)	81.07(7)	87.89(3)	90.51(2)	99.938(10)	100.026(1)	92.21(2)
γ (°)	86.39(5)	87.63(3)	90	90.934(10)	92.771(2)	90.030(13)
V (Å^3)	779.0(10)	772.5(3)	1652.4(9)	841.3(2)	730.96(8)	805.9(2)
no.collected intensities	2946	5599	2779	3903	4494	3523
no.unique intensities	2744	3538	2744	2978	1885	2108
no.observed intensities [a])	2073	2389	2734	1760	1453	1178
2Θ range (°)	50	55.4	50	50.2	46.5	45
R_{merg}	0.020	0.039	0.074	0.028	0.019	0.101
$D_{calc.}$ (g/cm^{-3})	1.336	1.261	1.312	1.328	1.224	1.291
Z	1	1	2	1	1	1
T (K)	170	140	130	298	293	298
R1 (obs. data)	0.046	0.074	0.062	0.060	0.062	0.078
wR2 (all data)	0.1272	0.220	0.252	0.184	0.180	0.248
μ (cm^{-1})	0.093	0.080	0.089	0.106	0.079	0.091
residualelectron density (e Å^{-3})	0.20	0.59	0.28	0.25	0.52	0.22
no. of parameters [b])	212	203	228	247	184	211
refinement comments [c])		[d])	[d])	[e])		
diffractometer [f])	Nicolet R3	Nicolet R3	Nicolet R3	Siemens P4	Smart/CCD [g])	Siemens P4

[a]) observation criteron I > 2σ(I) [b]) hydrogen atoms of the alkohols were located from difference Fourier analyses were treated as riding groups with free isotropic U-values, the other hydrogen atoms were positioned at calculated sites and refined as riding groups with the 1.2-fold of the corresponding C-atoms and the 1.5-fold for methyl groups. [c]) SHELXTL (Vers. 5.03) program package used for structure solving with Direct Methods and refinement on F^2. [d]) the oxygen atom O(1) was disordered over two sites, given occupancies of 0.9 and 0.1, respectively. [e]) the fluorine atoms of the CF_3 groups were disordered and were calculated with equal occupancies at torsion angles of 60° each. [f]) equiped with graphite monochromized Mo-K_α radiation [g]) detector distance 4.457 cm; the standard deviations calculated by the program for the cell dimensions are probably too small and should be multiplied by a factor of 2 – 10

to 5.732 Å (*Ib* in Table 2). The distances of aryl groups in different stacks (*Ia* in Table 2) are similar ranging from 5.324 to 5.870 Å. Although the separation of the centers of the aryl groups seem to be large, parts of the aryl groups are much closer to each other due to the tilted structure. Finally, it should be noted that the substituents in 4-position of the phenyl group, *i.e.* 4-nitro, 4-methoxycarbonyl, and 4-dimethylamino, are arranged in such a way that a perfect overlap of their π-electrons with those of the aromatic residue is achieved.

Cocrystals of meso-1,2-Bis(4-methoxyphenyl)-1,2-ethanediol (**3**) *and Bisimines* **4** and **7**

Among the possible combinations of **3** with **4** through **9** only two, those of the bisimines with the unsubstituted phenyl group (**4**) and of the bisimine with the 4-methoxycarbonyl substituted phenyl group (**7**), could be cocrystallised successfully. The crystal structure determined for (**3** + **7**) (Table 2 and 3) shows no peculiarities when compared to that of (**2** + **7**).

Spectroscopic Studies on Cocrystals of **2** and **3** *with* **5** *through* **8**, *respectively* **11**

UV/Vis spectra of the cocrystals were recorded in diffuse reflection mode. Figure 4 presents spectra of the cocrystals and of the individual components for (**2** + **5**), (**2** + **6**), and (**2** + **7**). It can easily be seen that the spectra of the cocrystals are not just the sum of the spectra of the individual components. In particular for (**2** + **6**) a new absorption band, interpreted as CT excitation, shows a discrete maximum at 465 nm which confers an orange-red colour to these cocrystals. In the other spectra a CT absorption appears as shoulder. For cocrystals (**2** + **9**) and (**3** + **7**) (spectra not shown) it is not possible to recognize an absorption which is different from the spectra of the components. It should be noted, however, that UV/Vis spectra recorded in diffuse reflection can not be discussed easily in a quantitative manner [15]. Thus, it is difficult to construct the expected UV/Vis spectrum without CT interactions as superposition of the spectra of the individual molecules.

Figure 5 shows UV/Vis spectra for (**2** + **5**) and (**3** + **7**) taken on pure cocrystals in diffuse reflection. The technique of recording was such that a layer of finely powdered potassium bromide was covered with a thin layer of small cocrystals without mixing. This is done for two reasons. Firstly, it was noticed that the properties of some cocrystals are influenced when they were thoroughly ground with potassium bromide, and secondly, this mode of operation proves to be superior for the study of the thermal reversibility of the photochromism. This latter point proves to be essential when comparing the results of the UV/Vis and the IR spectra. Visible and infrared light penetrate potassium bromide to a different extent, thus partially reaching molecules in different layers and therefore making the comparison of the results difficult.

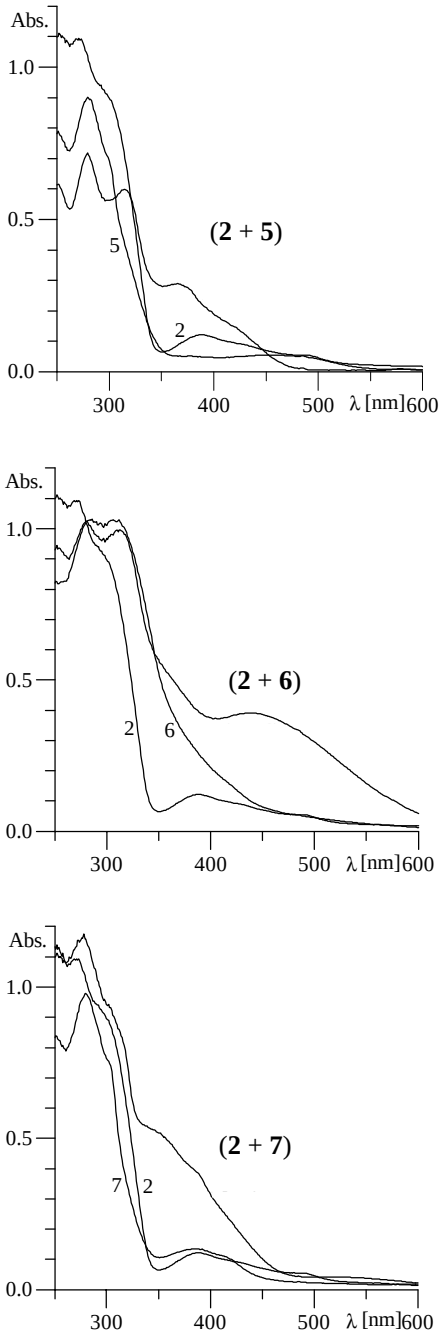

Fig. 4 UV/Vis spectra of the cocrystals of *meso*-1,2-bis(4-dimethylaminophenyl)-1,2-ethanediol (**2**) and 1,4-bisimines **5**–**7** in KBr (molar ratio 1 : 5 × 10^{-3}).

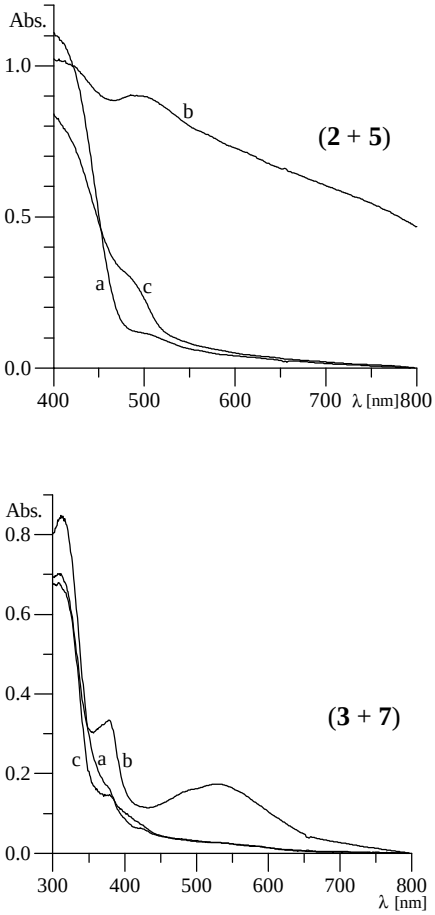

Fig. 5 UV/Vis spectra of the cocrystals of *meso*-1,2-bis(4-dimethylaminophenyl)-1,2-ethanediol (**2**) and bis(4-cyanobenzylidene)ethylenediamine (**2** + **5**) and of 1,2-bis(4-methoxyphenyl)-1,2-ethanediol and bis(4-nitrobenzylidene)ethylenediamine (**3** + **7**) in diffuse reflection on KBr, before (a) and after (b) irradiation, and after heating (c). For details see text.

The three traces for (**2** + **5**) in Figure 5 represent the spectrum of the cocrystals not exposed to light (a), the spectrum of the same sample irradiated with the light of a 1 kW Hg/Xe lamp (Schott UG5 and WG360 filters) for five seconds (b), and the spectrum of the same sample heated at ca. 90 °C for ca. 20 hours (c). The filter system makes sure that only light of λ > ca. 320 nm reaches the sample. On irradiation an almost uniform absorption without specific structure is found in the visible region. About one day at elevated temperatures (ca. 90 °C) is necessary to regain the original spectrum. The

photochromism is not completely reversible as can be recognized in trace c of Figure 5. This phenomenon is attributed to some photochemical degradation of the cocrystals. A ^{1}H NMR spectrum of dissolved cocrystals that had been previously irradiated shows that diol **2** is cleaved to 4-dimethylaminobenzaldehyde. The amount of cleavage increases with irradiation time. Therefore, we suggest that 4-dimethylaminobenzaldehyde is responsible for the residual absorption seen in trace c. Except for the influence of this side reaction the colour change can be repeatedly induced by light and reverted thermally. A comparable experiment with (**3** + **7**) is also shown in Figure 5. On irradiation (1 kW Hg/Xe lamp, Schott UG5 and WG 345 filters) for fifteen seconds two new absorption bands are generated, one rather narrow band at 380 nm and one broad band displaying a maximum at 540 nm. Trace c in Figure 5 shows the spectrum of the same sample after heating it to 65 °C for 17 h. The new absorptions have disappeared which demonstrates the reversibility of the photochromism. Similar results are obtained for the other cocrystals of **2** and acceptor-substituted bisimines. Cocrystal (**2** + **6**) behaves slightly different as changes in the UV/Vis spectrum require longer irradiation times.

It is interesting to analyse the IR spectra of both the irradiated and non-irradiated samples (Table 4). The spectra of the cocrystals not yet exposed to light are characterized by a broad absorption of the OH-vibration with peaks between 3 211 and 3 282 cm^{-1}. Further, each cocrystal exhibits an absorption at ca. 1 640 cm^{-1} which is attributed to the C=N-vibration of the bisimine by comparison with authentic samples. On irradiation, all cocrystals of **2** with **5**–**8**, respectively **11** and of **3** with **7** exhibit a new band or shoulder at ca. 3 350 – 3 400 cm^{-1} which grows out of the broad OH-vibration. These are interpreted as NH-vibrations. There are some additional changes in the IR spectra. All cocrystals develop an absorption at ca. 1 680 cm^{-1}. The IR spectrum of the cocrystal (**2** + **5**) provides further information [9]. It displays one band for the cyano vibration at 2 226 cm^{-1} when grown in the dark. On exposure to light for about five seconds (1 kW HG/Xe lamp, Schott UG5 and WG360 filters) an additional band of comparable intensity is generated at 2 177 cm^{-1}. Thus a new species is generated with a CN-vibration at smaller wave numbers than in the original spectrum. Qualitatively, the equal intensity of the two bands might indicate ca. 50% conversion of the cocrystals to a new state. The changes in the IR spectra which occur on irradiation are thermally reversible. The disappearance of the new absorptions on heating parallels the reversion of the UV/Vis spectra to the original state. The changes which remain after heating the crystals seem to be due to degradation products, for instance the absorption at 1680 cm^{-1} might be due to photochemical cleavage of the diol to a carbonyl compound.

The photochromism is not restricted to the complexes (**2** + **5**) and (**3** + **7**) as shown in Figure 5. Prototypal UV/Vis spectra obtained from samples which were prepared by thoroughly grinding potassium bromide and the respective cocrystal in a molar ratio of 1 : 5×10^{-3} are presented in Figure 6 prior to and after light exposure (1 kW Hg/Xe lamp (grid 34%, Schott UG5 filter). The cocrystal of *meso*-1,2-bis(4-dimethylaminophenyl)-1,2-ethanediol and bisimines **5** and **7** produce a new absorption at 360 nm. This absorption is absent if *meso*-1,2-bis(4-methoxyphenyl)-1,2-ethanediol **3** forms the cocrystal with **7** (spectrum not shown). Thus, we assume that the absorption at 360 nm is due to the new chromophore which is formed from *meso*-1,2-bis(4-dimethylaminophenyl)-1,2-ethanediol on irradiation. On the other hand the long wavelength absorptions seem to be due to the new chromophore formed from the bisimines.

All cocrystals from **2** and **5**–**8**, respectively **11**, and from **3** and **7** become paramagnetic on irradiation. A typical example is shown in Figure 7 for (**2** + **5**). The absorption is broad without fine structure and gradually increases in intensity with irradiation time. The g-values (Table 4) are typical for organic carbon centered radicals. For (**2** + **5**) we determined the number of unpaired spins quantitatively after reaching saturation of

Table 4 IR- and ESR-data of photochromic cocrystals

cocrystal	non-irradiated			irradiated			
	IR			IR (additional bands)			ESR
	OH	CH=N	other	N-H	C=O	other	g-value
(**2** + **5**)	3261	1648					
(**2** + **6**)	3274	1646	2226 (CN)	3355	1687	2177 (CN)	2.0033
(**2** + **7**)	3260	1640		3344	1664	1572	2.0035
(**2** + **8**)	3267	1648		3396	1674	1600 1376	2.0032
(**2** + **11**)	3282	1651		3358	1684	1600 [a]) 1550 [a]) 1168 [a])	2.0033
(**3** + **7**)	3211			3384	1684	1600 [a])	2.0031

[a]) increase in intensity of existing bands.

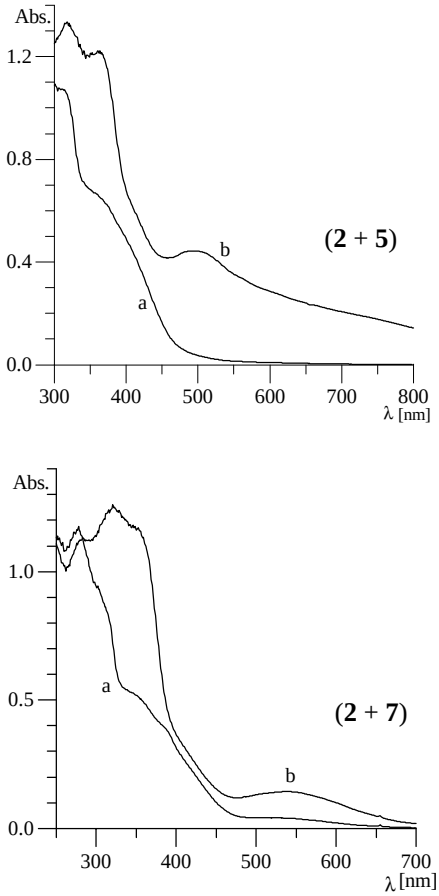

Fig. 6 UV/Vis spectra of cocrystals (**2** + **5**) and (**2** + **7**) in KBr matrix, before (a) and after (b) irradiation (molar ratio $1 : 5 \times 10^{-3}$).

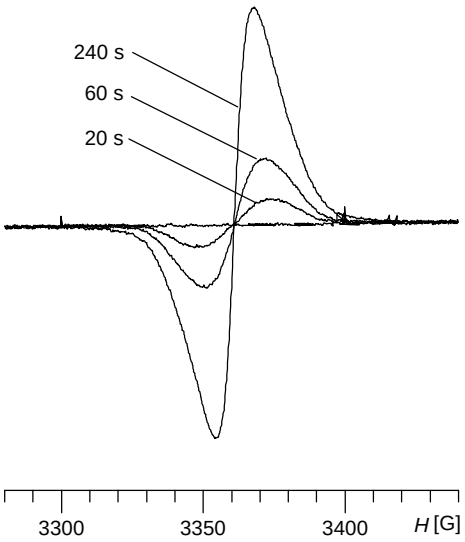

Fig. 7 ESR spectrum of cocrystals (**2** + **5**) as function of irradiation time.

the ESR signal intensity on prolonged irradiation [9]. A spin concentration of 30 – 40% was determined, indicating that 15 to 20 per cent of diol and bisimine had been converted to radical states. Quantitative measurements of spin concentrations by ESR spectroscopy should not be overemphasized, in particular when carried out on solid samples. For this reason we determined the spin concentration also by a SQUID measurement. A sample of the cocrystal was irradiated by a Hg/Xe-lamp (Schott UG5 and GG395 filters) until no further increase in the ESR signal intensity was observed. The crystals showed a spin concentration of 15%, in other words ca 8% of diol and bisimine are present as radicals. Considering the approximate character of the quantitative ESR determination the agreement between the two methods is satisfactory. The temperature dependent SQUID measurement indicated a normal Curie behaviour of the unpaired spins, thus not demonstrating special magnetic interactions. It should be noticed that the ESR signals vanish when the samples are heated at higher temperatures, *i.e.* the paramagnetism is also coupled to the photochromism.

Discussion

Only the *meso*, not the *D* or *L* form of unsubstituted or 4-substituted 1,2-diaryl-1,2-ethanediols yield cocrystals with differently substituted bis(arylidene)ethylenediamines. The presumption that CT interactions are generated when 4-donor substituted *meso* diols are cocrystallized with 4-acceptor- substituted bisimines has been confirmed. Furthermore photochromism has been established. It goes along with an electron transfer, presumably from donor substituted to acceptor substituted aryl groups. The photochromism, the changes in the IR spectra, and the paramagnetism are thermally reversible. Thus, the systems can be considered as optical devices which can be switched back thermally [16].

A molecular mechanism in terms of a light induced, thermally reversible electron–proton transfer rationalizes the observations. Light of suitable wave length induces a CT excitation. The excited state corresponds to a radical ion pair as Kochi has shown [17]. Normally, the excited state reverts to the ground state after very short periods of time. We assume that the primary excitation is followed by a proton transfer from an O–H group to the nitrogen of the bisimine. Thus, the excited state is trapped, and the radical anion becomes formally a neutral radical. Simultaneously, the radical cation becomes formally neutral, too. However, here the regions of positive and negative charges are still separated by sp^3 hybridized C-atoms which prevents the system from charge compensation.

The reversion to the starting state needs thermal activation although it might be argued that the process corresponds simply to a migration of a proton from nitrogen to oxygen in a suitable arrangement. The thermal

activation seems to be necessary because the proton migration leads to a radical anion and a radical cation which corresponds to the original excited CT state. This excited state, possibly in a distorted geometry, then deactivates leading to the initial ground state. All attempts to detect alterations in the crystal structure by X-ray diffraction failed, presumably because of the small turn over on irradiation.

Photochromism is a well known and carefully investigated process [18]. If we wish to relate our results to other cases, we may find some similarities with the photochromism of salicylideneanils [19]. These compounds, which can also be thermochromic, undergo an *E/Z* isomerization and a proton transfer from oxygen to nitrogen after intramolecular photo excitation. This phenomenon, coupled to the solid state, is also thermally reversible. Our examples are different in so far as an intermolecular photo excitation precedes an intermolecular proton transfer.

This work was supported by the Deutsche Forschungsgemeinschaft and the Fonds der Chemischen Industrie. Prof. K. Wieghardt and Dr. E. Rentschler, Max-Planck-Institut für Strahlenchemie, Mülheim kindly carried out the SQUID measurement.

Experimental

All reactions were carried out in dry solvents. Melting points are uncorrected. IR Spectra: Perkin-Elmer FT-IR 1600 spectrometer and BIO-RAD FT-IR-Spectrometer, FT 135. ^{1}H NMR and ^{13}C NMR-Spectra: Gemini 200 or Bruker AMX 300 (TMS as internal standard). Mass spectra: VG ProsSpec 3000. ESR: Bruker ER 420. UV spectra: J&M-spectrometer, Tidas. 4-Cyano-, 4-nitro-, 4-trifluormethyl-, 4-pyridyl-, dimethylamino-, methoxybenzaldehyde and *meso*-1,2-diphenylethandiol (**1**) are commercial substances. 4-Carbomethoxybenzaldehyde was prepared from 4-carboxybenzaldehyde with methanol. *Meso*-1,2-bis(4-dimethylaminophenyl)-1,2-ethanediol (**2**) [20, 21] and *meso*-1,2-bis(4-methoxyphenyl)-1,2-ethanediol (**3**) [20, 21] were prepared according to literature procedures.

Preparation of Bisimines (General Procedure)

60 mmol of aldehyde and 30 mmol ethylendiamine were dissolved in 100 ml toluene and 3.0 g molecular sieve (3Å) was added. After 24 h the molecular sieve was removed by filtration, and the solvent was distilled off *in vacuo*. The crude product was recrystallized from ethylacetate.

N,N'-Bis(4-nitrobenzylidene)ethylenediamine (**6**)

8.8 g (90%) from ethylacetate. *m.p.* 189–190 °C. – ^{1}H NMR (200 MHz, $CDCl_3$): δ/ppm = 3.99 (s, 2H; CH_2), 7.77–8.20 (d,d, ^3J(H,H) = 8.8 Hz, 4H, aromatic-H), 8.31 (s, 1H; CH). – ^{13}C NMR (50 MHz, $CDCl_3$): δ/ppm = 61.48 (CH_2), 123.95, 128.82, 141.45, 149.20 (aromatic-C), 160.44 (CH). – IR (KBr): $\tilde{\nu}$/cm^{-1} = 1644 (C=N). – UV/VIS (KBr): λ_{max}/nm (Abs) = sh 249 (0.81), 284 (1.03), 308 (1.02). – MS (70eV, EI): *m/z* (%): 327 (27) [M$^+$ + H], 297 (12), 178 (100), 163 (40) [1/2M$^+$], 149 (45);

$C_{14}H_{14}N_4O_4$	Calcd.:	C 58.89	H 4.32	N 17.17
(326.3)	Found:	C 59.09	H 4.34	N 16.93.

N,N'-Bis(4-cyanobenzylidene)ethylenediamine (**5**)

7.9g (93%) from ethylacetate. *m.p.* 239 °C. – ^{1}H NMR (300 MHz, $CDCl_3$): δ/ppm = 4.00 (s, 2H; CH2), 7.64–7.79 (d,d, ^3J(H,H) = 8.3 Hz, 4H, aromatic-H), 8.29 (s, 1H; CH). – ^{13}C NMR (75 MHz, $CDCl_3$): δ/ppm = 61.40 (CH_2), 114.02, 129.89, 132.90, 139.73 (aromatic-C), 118.43 (CN), 160.72 (CH). – IR (KBr): $\tilde{\nu}$/cm^{-1} = 2 226 (CN), 1 643 (C=N). – UV/VIS (KBr): λ_{max}/nm (Abs) = 252 (0.78), 280 (0.89), sh 300 (0.69). – MS (70eV, EI): *m/z* (%): 287 (25) [M$^+$ + H], 158 (82), 143 (54) [1/2 M$^+$], 129 (70), 116 (100);

$C_{18}H_{14}N_4$	Calcd.:	C 75.50	H 4.93	N 19.57
(286.3)	Found:	C 75.48	H 4.84	N 19.50.

N,N'-Bis(4-carboxymethoxybenzylidene)ethylenediamine (**7**)

8.3g (79%) from ethylacetate. *m.p.* 170 °C. – ^{1}H NMR (300 MHz, $CDCl_3$): δ/ppm = 2.14 (s, 3H, CH_3), 3.99 (s, 2H; CH_2), 7.71–8.03 (d,d, ^3J(H,H) = 8.7Hz, 4H, aromatic-H), 8.29 (s, 1H; CH). – ^{13}C NMR (75 MHz, $CDCl_3$): δ/ppm = 52.59 (CH_3), 61.49 (CH_2), 127.92, 129.82, 131.81, 139.84 (aromatic-C), 161.84 (CH), 166.61 (CO_2R). – IR (KBr): $\tilde{\nu}$/cm^{-1} = 1722 (C=O), 1638 (C=N). – UV/VIS (KBr): λ_{max}/nm (Abs) = 251 (0.84), 279 (0.98), sh 303 (0.75), 385 (0.13). – MS (70eV, EI): *m/z* (%): 353 (6) [M$^+$ + H], 201 (75), 186 (55) [1/2 M$^+$], 172 (72), 159 (100).

$C_{20}H_{20}N_2O_4$	Calcd.:	C 68.17	H 5.71	N 7.95
(352.4)	Found:	C 68.17	H 5.68	N 7.92.

N,N'-Bis(4-trifluormethylbenzylidene)ethylendiamine (**8**)

9.1g (81%) from ethylacetate. *m.p.* 114 °C. – ^{1}H NMR (200 MHz, $CDCl_3$): δ/ppm = 4.02 (s, 2H; CH_2), 7.26–7.82 (d,d, ^3J(H,H) = 8.0Hz, 4H, aromatic-H), 8.32 (s, 1H; CH). – ^{13}C NMR (50 MHz, $CDCl_3$): δ/ppm = 62.03 (CH_2), 121.84 (CF_3), 126.25, 128.91, 132.61, 139.80 (aromatic-C), 161.84 (CH). – IR (KBr): $\tilde{\nu}$/cm^{-1} = 1644 (C=N). UV/VIS (KBr): λ_{max}/nm (Abs) = 251 (0.81), 279 (0.78), sh 288 (0.71), sh 310 (0.35). MS (70eV, EI): *m/z* (%): 373 (8) [M$^+$ + H], 353 (6), 201 (95), 186 (62), 172 (82, 159 (100).

$C_{18}H_{14}N_2F_6$	Calcd.:	C 58.07	H 3.79	N 7.52
(334.3)	Found:	C 58.15	H 3.70	N 7.44.

N,N'-Bis(4-pyridylmethylen)ethylenediamine (**11**)

5.3g (75%) from ethylacetate. *m.p.* 130 °C. – ^{1}H NMR (300 MHz, $CDCl_3$): δ/ppm = 3.99 (s, 2H; CH_2), 7.49 (d, ^3J(H,H) = 6.0 Hz, 2H, aromatic-H), 8.22 (s, 1H; CH), 8.63 (d, ^3J(H,H) = 6.0 Hz, 2H, aromatic-H). – ^{13}C NMR (75 MHz, $CDCl_3$): δ/ppm = 61.22 (CH_2), 121.78, 142.57, 150.38 (aromatic-C), 160.79 (CH). IR (KBr): $\tilde{\nu}$/cm^{-1} = 1648 (C=N). UV/VIS (KBr): λ_{max}/nm (Abs) = 248 (0.82), 280 (0.83), 378 (0.28). – MS (70eV, EI): *m/z* (%): 239 (1) [M$^+$ + H], 134 (50), 119 (56) [1/2 M$^+$]9-, 105 (16), 83 (100).

$C_{14}H_{14}N_4$	Calcd.:	C 70.56	H 5.92	N 23.51
(238.3)	Found:	C 70.57	H 5.81	N 23.80.

N,N'-Bis(4-dimethylaminobenzylidene)ethylenediamine (**9**)

6.2 g (70%) from ethylacetate. *m.p.* 172–173.5 °C. – ^{1}H-NMR (300 MHz, $CDCl_3$): δ/ppm = 3.86 (s, 4H; CH_2), 6.66 (d, ^3J =

9 Hz, 4H; aromatic-H), 7.56 (d, ^3J = 9 Hz, 4H; aromatic-H), 8.15 (s, 2H; CH). – ^{13}C NMR (75 MHz, $CDCl_3$): δ/ppm = 40.19 (CH_3), 62.06 (CH_2), 111.52, 124.46, 129.43, 151.90 (aromatic-C), 162.34 (CH). – IR (KBr): $\tilde{\nu}$/cm^{-1} = 1 639 (C=N). – MS (70 eV, EI): *m/z* (%): 322 (37) [M$^+$], 175 (83), 161 (100), 148 (78).

$C_{20}H_{26}N_4$	Calcd.:	74.50	H 8.12	N 17.37
(322.4)	Found:	C 74.60	H 8.00	N 17.36.

N,N'-Bis(4-methoxybenzylidene)ethylenediamine (**10**)

6.0 g (68%) from ethylacetate. *m.p.* 96 °C. – ^{1}H-NMR (300 MHz, $CDCl_3$): δ/ppm = 3.81 (s, 3H; CH_3), 3.88 (s, 4H; CH_2), 6.88 (d, ^3J = 8.79 Hz, 4H; aromatic-H), 7.62 (d, ^3J = 8.79 Hz, 4H; aromatic-H), 8.19 (s, 2H; CH). – ^{13}C NMR (75 MHz, $CDCl_3$): δ/ppm = 55.31 (CH_3), 61.68 (CH_2), 113.89, 129.10, 129.62, 131.99 (aromatic-C), 161.97 (CH). – IR (KBr): $\tilde{\nu}$/cm^{-1} = 1637 (C=N). – MS (70 eV, El): *m/z* (%): 297 (25) [M$^+$ + 1], 163 (100), 148 (50).

meso-1,2-Bis(4-dimethylaminophenyl)-1,2-ethanediol (**2**)

m.p. 178 °C, (Lit. [21]): *meso*: 178–179 °C). – ^{1}H NMR (300 MHz, $CDCl_3$): δ/ppm = 2.90 (s, 12H; CH_3), 4.63 (s, 2H; CH), 6.60 (d, ^3J = 9 Hz, 4H; aromatic-H), 7.04 (d, ^3J = 9 Hz, 4H; aromatic-H). – ^{13}C NMR (75 MHz, $CDCl_3$): δ/ppm = 40.63 (CH_3), 78.62 (CH), 112.28, 124.20, 129.79, 150.06 (aromatic-C). – IR (KBr): $\tilde{\nu}$/cm^{-1} = 3338 (O–H), 1032 (C–O). – UV/VIS (KBr): λ_{max}/nm (Abs) = 252 (1.10), 271 (1.08), sh 301 (0.87), 388 (0.11).

meso-1,2-Bis(4-methoxyphenyl)-1,2-ethanediol (**3**)

m.p. 165 °C (EtOH), (Lit. [21]: 172 °C). ^{1}H NMR (300 MHz, $CDCl_3$): δ/ppm = 3.73 (s, 6H; CH_3), 4.66 (s, 2H; CH), 6.69 (d, ^3J = 6.6 Hz, 4H; aromatic-H), 7.04 (d, ^3J = 6.6 Hz, 4H; aromatic-H). – ^{13}C NMR (75 MHz, $CDCl_3$): δ/ppm = 55.25 (CH_3), 77.78 (CH), 113.68, 128.31, 131.98, 159.42 (aromatic-C). – IR (KBr): $\tilde{\nu}$ /cm^{-1} = 3 344, 3 278 ((O–H), *meso*-Diol), 1 256 ((C–O), Arylether), 1 028 (C–O). – UV/VIS (KBr): $\lambda_{max/nm}$ (Abs) = 238 (0.51), 276 (0.64), 283 (0.65), 310 (0.28), sh 329 (0.23), 348 (0.16). – MS (70 eV): *m/z* [%]: 274 (< 1) [M$^+$], 257 (6) [M$^+$ – OH], 137 (100).

Preparation of Cocrystals All cocrystals were grown from a hot saturated ethylacetate solution of a equimolar mixture of the bisimine and the corresponding *meso*-1,2-bisphenyl-1,2-ethanediol in the dark.

N,N'-Bis(4-nitrobenzylidene)ethylenediamine (**6**)*/meso-Bis(4-dimethylamino)phenyl-1,2-ethanediol* (**2**)

red needles, *m.p.* 201–203 °C. – IR (KBr): $\tilde{\nu}$/cm^{-1} = 3 261 (OH), 1 649 (C=N). – UV/VIS (KBr): λ_{max}/nm (Abs) = 252 (0.94), 280 (1.02), 311 (0.99), 443 (0.39).

N,N'-Bis(4-cyanodibenzylidene)ethylenediamine (**5**)*/meso-1,2-Bis(4-dimethylamino)phenyl-1,2-ethanediol* (**2**)

yellow needles, *m.p.* 211 °C, IR (KBr): $\tilde{\nu}$/cm^{-1} = 3 271 (OH), 1 646 (C=N). – UV/VIS (KBr): λ_{max}/nm (Abs) = 251 (0.61), 279 (0.71), 315 (0.59), 366 (0.28), sh 406 (0.17).

N,N'-Bis(4-carbomethoxybenzylidene)ethylenediamine (**7**)*/meso-1,2-Bis(4-dimethylamino)-phenyl-1,2-ethanediol* (**2**)

yellow needles, *m.p.*193 °C, IR (KBr): $\tilde{\nu}$/cm^{-1} = 3 260 (OH), 1 640 (C=N). – UV/VIS (KBr): λ_{max}/nm (Abs) = 252 (1.14), 278 (1.17), sh 302 (0.94), sh 352 (0.51), sh 387 (0.39).

N,N'-Bis(4-trifluormethylbenzylidene)ethylenediamine (**8**)*/meso-1,2-Bis(4-dimethylamino)-phenyl-1,2-ethanediol* (**2**)

yellow needles, *m.p.*188 °C. – IR (KBr): $\tilde{\nu}$/cm^{-1} = 3 265 (OH), 1 648 (C=N). – UV/VIS (KBr): λ_{max}/nm (Abs) = 250 (0.90), 2787 (0.87), 312 (0.82), sh 363 (0.39), sh 438 (0.11).

N,N'-(4-Pyridylmethylene)ethylenediamine (**11**)*/meso-1,2-Bis(4-dimethylamino)phenyl-1,2-ethanediol* (**2**)

yellow needles, *m.p.* 179 °C. – IR (KBr): $\tilde{\nu}$/cm^{-1} = 3 282 (OH), 1 651 (C=N). – UV/VIS (KBr): λ_{max}/nm (Abs) = 249 (0.92), 275 (0.90), 308 (0.79), sh 36 (0.38).

N,N'-Bis(benzylidene)ethylenediamine (**4**) *[22]/meso-Bis(4-dimethylaminophenyl)-1,2-ethanediol* (**2**)

light yellow needles, *m.p.* 128 °C. – IR (KBr): $\tilde{\nu}$/cm^{-1} = 3 273 (OH), 1 643 (C=N).

N,N'-Bis(4-carbomethoxybenzylidene)ethylenediamine (**7**)*/meso-1,2-Bis(4-methoxyphenyl)-1,2-ethanediol* (**3**)

achromatic small plates; *m.p.* 159–160 °C. – IR (KBr): $\tilde{\nu}$/cm^{-1} = 3 211 (OH), 1 639 (C=N). – UV/VIS (KBr): λ_{max}/nm (Abs) = 255 (1.07), 277 (1.20), sh 300 (0.89), sh 352 (0.24), sh 376 (0.14).

N,N'-Bis(benzylidene)ethylenediamine (**4**)*[22]/meso-1,2-Bis(4-methoxyphenyl-1,2-ethanediol* (**3**)

achromatic crystals, *m.p.* 129–138 °C. – IR (KBr): $\tilde{\nu}$/cm^{-1} = 3 222 (OH), 3 444 sh, 1 639 (C=N).

N,N'-Bis(4-nitrobenzylidene)ethylenediamine (**6**)*/meso-1,2-Diphenyl-1,2-ethanediol* (**1**)

orange needles; *m.p.* 172 °C. – IR (KBr): $\tilde{\nu}$/cm^{-1} = 3 199 (OH), 1 646 (C=N).

N,N'-Bis(4-carbomethoxybenzylidene)ethylenediamine (**7**)*/meso-1,2-Diphenyl-1,2-ethanediol* (**1**)

achromatic needles: *m.p.* 179 °C. – IR (KBr) $\tilde{\nu}$/cm^{-1} = 3 190 (OH), 1 724 (C=O), 1 647 (C=N).

N,N'-Bis(4-trifluoromethylbenzylidene)ethylenediamine (**8**)*/meso-1,2-Diphenyl-1,2-ethanediol* (**1**)

achromatic needles, *m.p.* 130 °C. – IR (KBr): $\tilde{\nu}$/cm^{-1} = 3 222 (OH), 1 649 (C=N).

N,N'-Bis(4-pyridylmethylen)ethylenediamine (**11**)*/meso-1,2-Diphenyl-1,2-ethanediol* (**1**)

light yellow small crystals; *m.p.* 120 °C. – IR (KBr): $\tilde{\nu}$/cm^{-1} = 3 226 (OH), 1 646 (C=N).

N,N'-Bis(4-dimethylaminobenzylidene)ethylenediamine (**9**)*/meso-1,2-Diphenyl-1,2-ethanediol* (**1**)

light yellow small plates; *m.p.* 187–195 °C. – IR (KBr): $\tilde{\nu}$/cm^{-1} = 3 104, 3 131 (OH), 1 623 (C=N).

N,N'-Bis(4-methoxybenzylidene)ethylenediamine (**10**)*/meso-1,2-Diphenyl-1,2-ethanediol* (**1**)

achromatic crystals, *m.p.* 150 °C. – IR (KBr): $\tilde{\nu}$/cm^{-1} = 3 314 (sh), 3 182 (OH), 1 648 (C=N).

References

[1] G. A. Jeffrey, W. Saenger, Hydrogen Bonding in Biological Structures, Springer Verlag, Berlin 2. Aufl. 1994, p-169-411
[2] J. M. Lehn, Supramolecular Chemistry, VCH, Weinheim 1. Aufl. 1995
[3] G. R. Desiraju, Angew. Chem. 1995, *107*, 2541; Angew. Chem. Int. Ed. Engl. **1995**, *34*, 2328
[4] J. C. MacDonald, G. M. Whitesides, Chem. Rev. **1994**, *94*, 2382
[5] D. S. Lawrence, T. Jiang, M. Levett, Chem. Rev. **1995**, *95*, 2229
[6] T. Smolka, R. Sustmann, R. Boese, J. Prakt. Chem. **1999**, *341*, 378
[7] A. Reyes-Arellano, R. Boese, I. Steller, R. Sustmann, Struct. Chem. **1995**, *6*, 391
[8] for a review see: C. A. Hunter, Chem. Soc. Rev. **1994**, 101
[9] M. Felderhoff, I. Steller, A. Reyes-Arellano, R. Boese, R. Sustmann, Adv. Mater. **1996**, *8*, 402
[10] W. T. Pennington, S. Chakraborty, I. C. Paul, D. Y. Curtin, J. Am. Chem. Soc. **1988**, *110*, 6498
[11] G. Briegleb, Elektronen-Donator-Acceptor-Komplexe, Springer Verlag, Berlin 1. Aufl. 1961, p 175 – 181
[12] Crystallographic data for the structures reported in this paper have been deposited with the Cambridge Crystallographic Data Centre as supplementary publications: CCDC-132537 (**2** + **5**), CCDC-132538 (**2** + **6**), CCDC-132539 (**2** + **7**), CCDC-132540 (**2** + **8**), CCDC-132541 (**2** + **11**), CCDC-132542 (**3** + **7**). Copies of the data can be obtained free of charge on application to CCDC, 12 Union Road, Cambridge CD2 IEZ, UK.
[13] J. Bernstein, M. C. Etter, L. Leiserowitz, in Structure Correlation (Eds.: H.-B. Bürgi, J. D. Dunitz), VCH, Weinheim 1. Aufl. 1994, p. 413 – 507
[14] G. Geiseler, H. Seidel, Die Wasserstoffbrückenbindung, Vieweg, Braunschweig, Berlin 1. Aufl. 1977, p. 139 – 173
[15] G. Kortüm, Reflexionsspektroskopie, Springer Verlag, Heidelberg-New York 1. Aufl. 1969, p. 180 – 192
[16] B. L. Feringa, W. F. Jager, B. de Lange, Tetrahedron **1993**, *49*, 8267
[17] E. F. Hilinsky, J. M. Masnovi, J. K. Kochi, P. M. Rentzepis, J. Am. Chem. Soc. **1984**, *106*, 8071
[18] Photochromism (Eds.: H. Dürr, H. Bouas-Laurent), Elsevier, Amsterdam 1. Aufl. 1990, p. 15 – 712
[19] M. D. Cohen, G. M. J. Schmidt, J. Phys. Chem. **1962**, *66*, 2442; M. D. Cohen, G. M. J. Schmidt, Flavian, J. Chem. Soc. **1964**, 2041; P. F. Barbara, P. M. Rentzepis, L. E. Brus, J. Am. Chem. Soc. **1980**, *102*, 2786
[20] J. M. Khurana, A. Sehgal, A. Gogia, A. Manian, G.C. Maikap, J. Chem. Soc., Perkin Trans. 1, **1996**, 2213
[21] A. Fürstner, R. Csuk, C. Rohrer, H. Weidmann, J. Chem. Soc. Perkin Trans. I **1988**, 1729
[22] H. A. Staab, F. Vögtle, Chem. Ber. **1965**, *98*, 2681

Address for correspondence:
Prof. Dr. R. Sustmann
Institut für Organische Chemie
Universität Essen
Universitätsstr. 5
D-45117 Essen
Fax: Internat. code (0)201-1834259
e-mail: sustmann@oc1.orgchem.uni-essen.de